Trans Indian Inst Met (2023) 76(7):1731–1740
https://doi.org/10.1007/s12666-023-02883-8

ORIGINAL ARTICLE

Low Temperature Pack Aluminising Process Effect on Ti6Al4V Alloy: Formation, Characterization and Oxidation Performances

Tuba Yener[1] · Ferhat Yılmaz[1] · Gozde Celebi Efe[2]

Received: 25 October 2022 / Accepted: 16 January 2023 / Published online: 10 February 2023

Abstract To improve the oxidation resistance of Ti6Al4V super alloy, an aluminide coating was deposited onto the surface. Without using a protective environment, the aluminising process was carried out for 4 and 6 h at 600, 700, and 800 °C temperatures. Subsequently, at 800 °C for 4, 20, and 40 h, the oxidation behavior of pack cemented aluminising coatings on Ti6Al4V was examined. The pack aluminising method was used to establish a uniform and continuous coating layer by the diffusion of aluminium into the Ti6Al4V super alloy. An intimate contact between the smooth, dense, porosity free coating layer and the matrix was identified. Dominant phase was detected as $TiAl_3$. After oxidation process Al_2O_3 phase was identified by XRD analysis along with TiAl3. The thickness of the layer was measured from the surface to the matrix and ranged from 0.5 to 20 µm, depending on the time and temperature of the process. To the SEM-Map analysis, oxide scale predominantly composed of Al_2O_3 for aluminised samples whereas TiO_2 was determined for bare sample. For aluminized samples, the development of the alumina layer provided greater protection for up to 40 h.

Keywords Ti6Al4V · Microstructure · Hardness · Oxidation · Aluminising

✉ Tuba Yener
tcerezci@sakarya.edu.tr

[1] Department of Metallurgy and Materials Engineering, Faculty of Engineering, Sakarya University, Sakarya, Turkey

[2] Department of Metallurgy and Materials Engineering, Technology Faculty, Sakarya University of Applied Sciences, Serdivan, Turkey

1 Introduction

Ti-6Al-4V alloy, α + β alloy that accounts for 45 percent of titanium alloys, is used in the automotive, aerospace, and biomedical industries because of its excellent properties, such as good corrosion resistance, high toughness, low density, and high strength [1], However, the production of Ti-6Al-4V alloys has a number of drawbacks, including manufacture cost [1–4]. Another inferior property of this alloy is; above 400 °C, the creep and wear resistance of Ti-6Al-4V alloy decreases. Coatings, such as aluminizing, chroming, and siliconizing are used to boost the creep and wear resistance of the metals [5]. Due to their high aluminium content and outstanding thermal stability, Al-X type coatings such as Al-Si, Al-Nb, and Al-Cr are extensively utilized as one of the most helpful high-temperature oxidation prevention coatings for titanium alloys and titanium aluminides [6].

Utilizing Al and Cr elements can improve the oxidation resistance of the coatings. They impart oxidation resistance thanks to the formation of a more stable oxide compared to iron oxides. These kind of elements protect the surface from the atmosphere by forming thin stable oxide films such as Al_2O_3, Cr_2O_3, SiO_2 [7]. To increase surface qualities due to environmental effects, a variety of strategies might be listed. Physical vapour deposition (PVD), thermal sputtering, plasma electrolytic oxidation and chemical vapor deposition (CVD) [8] are among the most commonly used processes for these coatings. Because of the cost of these techniques, studies have concentrated on cost-effective coating techniques. The pack aluminising process is an alternative way of coating alloy steels with hard and protective layer like aluminide to increase surface qualities including wear and corrosion resistance, friction, and oxidation resistance [9, 10]. The pack cementation method, like the CVD approach, can be

used to produce massive volumes of low-cost super alloys and steels in a variety of forms and sizes. Pack cementation technologies have a wide range of applications and allow for the uniform coating of objects with varying geometries, as well as being cost-effective and environmentally safe [11].

The aim of this study is to produce aluminised coated Ti6Al4V alloy via cheap and effective pack cementation technique to achieve high temperature oxidation resistance for higher oxidation temperatures.

2 Experimental

The substrate material was Ti6Al4V alloy with the dimensions of $30 \times 19.5 \times 2$ mm. Table 1 shows the chemical composition of the Ti6Al4V alloy used in this study. After surface cleaning by SiC grinding paper up to 1200 grit polishing was carried out with 1 µm Al_2O_3 suspension. Subsequently samples were placed into pack aluminizing powder container containing aluminium, NH_4Cl activator and Al_2O_3 filler material. The aluminising process was carried out in an atmospheric type furnace at 600, 700, and 800 °C for 4 and 6 h, respectively. Metallographic techniques and X-ray diffraction analyses were used to confirm the presence of the aluminides produced on the Ti6Al4V substrate (XRD). A Rigaku X-ray diffractometer (DMAX 2200) with a Cu Kα radiation source equipped with the wavelength of 1.541 Angstrom was used to characterize the phase of the deposited layer of the aluminised samples over a range of 20° to 80°. To detect the distribution of alloying components, scanning electron microscope (SEM, Model JEOL JSM-6060, Japan) equipped with energy dispersive spectroscopy (EDS) was used to evaluate the dispersion of phases in the coating layer. A Vickers type diamond indenter with a weight of 15 g and a dwell period of 10 s was used to determine the specimens' micro-hardness values.

Oxidation experiments were performed at 800 °C (Isothermal) for 4, 20, and 40 h in an open atmospheric type electric furnace (Protherm PLF 130/20). Subsequently, samples were analyzed utilizing XRD, SEM, and EDS analyses after the oxidation tests.

3 Results and Discussion

3.1 SEM–EDS and XRD Analyses

As the temperature and time used in the aluminizing process rises, the thickness of the coating layer expands, as can be observed in the cross-sectional microstructure. When looking at the microstructure of the coatings, it is determined that all aluminide coatings are made up of three layers (Fig. 1). The first phase formed on the top section on the coated layer has been identified to be $TiAl_3$ based on the SEM–EDS analysis shown in Fig. 2. Due to the rise in temperature and time, the coating thickness reached to 20 µm from the thinnest coating layer of roughly 0.5 µm. The second phase region corresponds to $TiAl_2$ intermetallic phase composition according to Ti-Al phase diagram. Figure 3 shows that the outmost layer deposited on the alloy contacted region is expected to be Ti_3Al intermetallic phase. The lowest temperature for aluminising applied for 4 h at 600 °C was not sufficient for the coating layer deposition, however, a thin intermetallic deposition was observed when the time increased to 6 h. Yang et al. [4]; studied growth kinetics of aluminide coating layers on Ti6Al4V alloy and similarly it is not seen a deposited layer for 600 °C-6 h process.

On the other hand, 800 °C caused the deterioration with a porous oxide layer formed on the surface. For this reason,

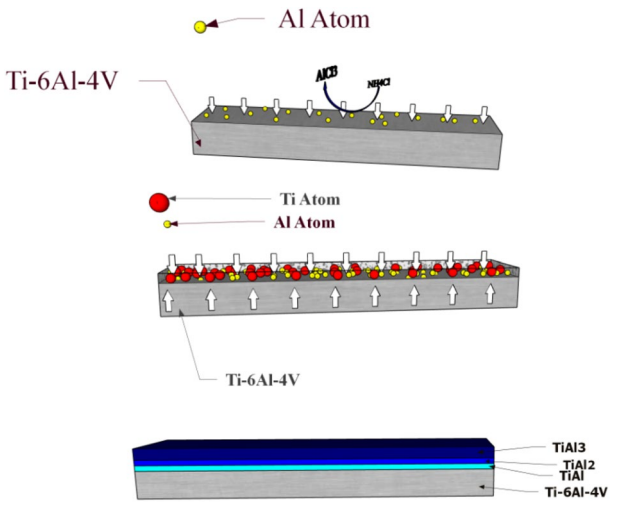

Fig. 1 Scheamatic representation of Al deposition on Ti6Al4V sample

Table 1 Composition of the Ti6Al4V alloy

Ele. (wt.%)	Ti	Al	V	H	Fe	O	C	N
Ti6Al4V	Balance	5.89	3.93	0.00198	0.165	0.128	0.0017	0.005

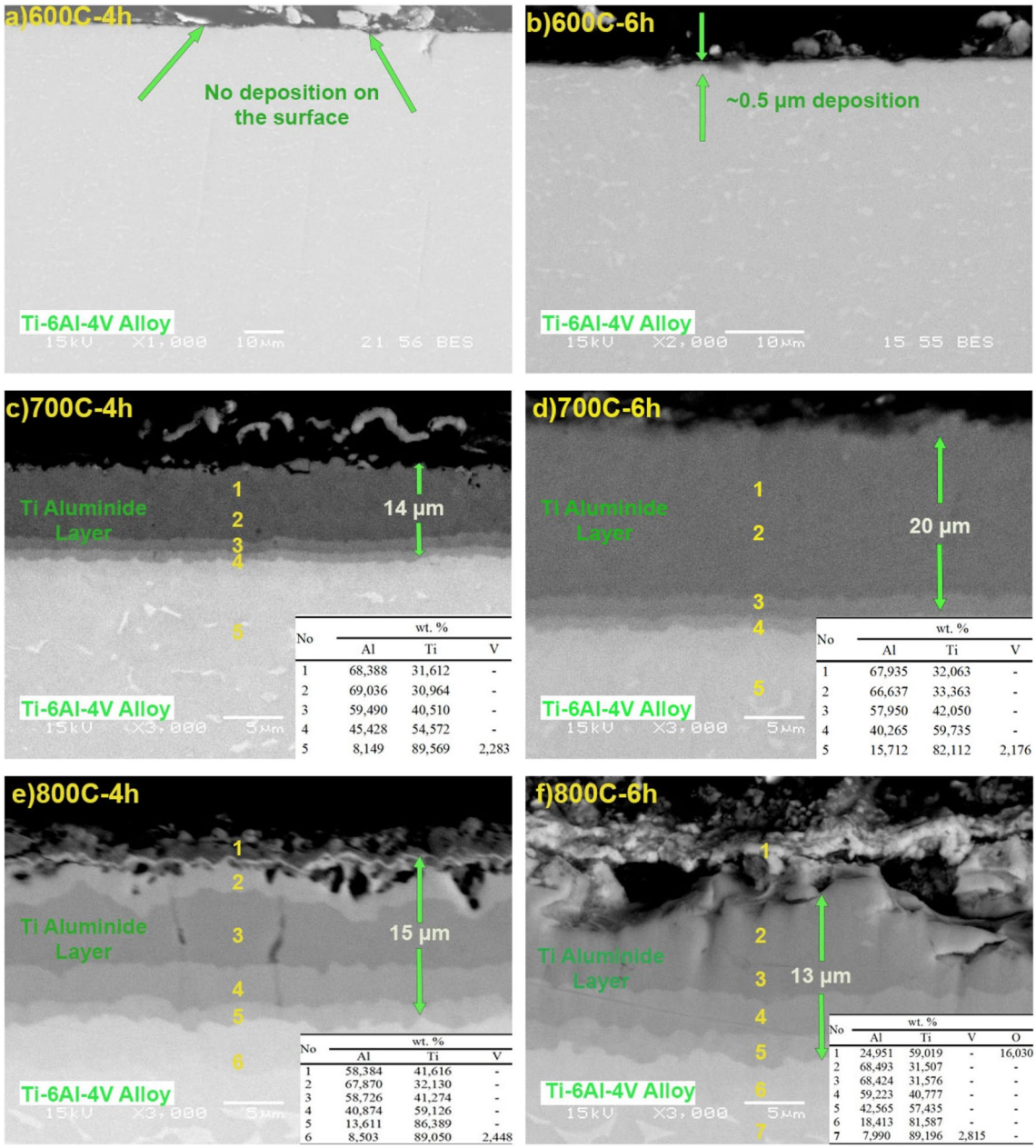

Fig. 2 SEM micrographs of low temperature pack aluminized Ti6Al4V Alloy; (a-b) 600 °C-4.6 h, (c-d) 700°4.6 h, (e–f) 800 °C-4.6 h

relatively low temperature aluminising durations at 700 °C for 4 and 6 h were determined as ideal for oxidation study.

The formation of titanium-aluminium-based intermetallic phases in the pack aluminising process can be seen as in Fig. 3. These phases are Ti_3Al, TiAl, $TiAl_2$, Ti_2Al_5, and $TiAl_3$ may be formed according to Ti-Al Phase diagram.

XRD analyses results of aluminized Ti6Al4V alloy can be seen in Fig. 4, The major phase composition of titanium aluminide phases consisted of $TiAl_3$ and $TiAl_2$. Some minor Ti, Al intermetallic phases were also identified. Although pack aluminising process was performed in open atmospheric conditions, it was only a trace amount oxide formation detected among the phases. However, 800 °C process time resulted some oxidation problem on the sample surface.

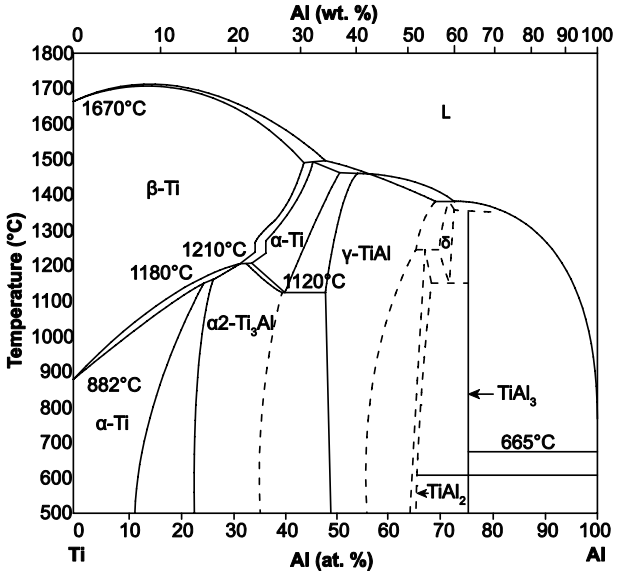

Fig. 3 Ti-Al Phase Diagram [12]

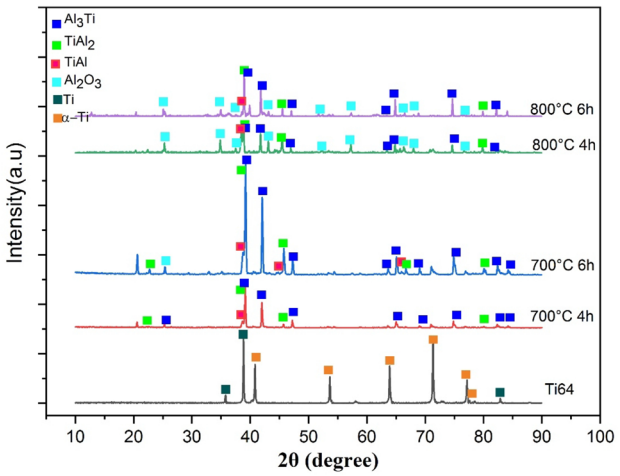

Fig. 4 XRD Analyses of aluminized Ti6Al4V sample

3.2 Hardness

The hardness graphs from distance to interior for the aluminised (Ti-Al-based intermetallic-coated) samples produced with the pack aluminizing process is shown in Fig. 5. On top surface of the coated sample an Al-rich $TiAl_3$ layer was formed in the coating, which was coated for 4 h at 700 °C, and its hardness was at around 600 HV. Similarly, a close value was obtained for the sample, produced at 700 °C for 6 h. Although the coating layer was wider in the sample produced in 6 h, more intense

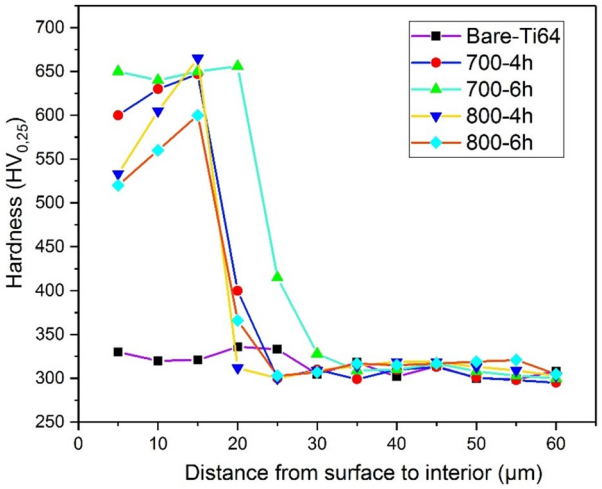

Fig. 5 Hardness graph of Al coated Ti6Al4V alloy

deposition was observed and the hardness value, reached 650 HV. Rastkar et al. [13] showed that as a result of aluminum coating of Ti-45Al-2Nb-2Mn-1B titanium alloy with plasma pack aluminising method at a temperature of 750 °C, the hardness values obtained from the TiAl3-based coating surface were similar to our study in which the hardness of the surface layers was up to 600 HV, which was higher than that of Ti-45Al-2Nb-2Mn-1B substrate (330 HV). In another study done by Yener et al. [14], $TiAl_3$ phase hardness was determined as 650 HV around for bulk material. Ti–rich intermetallics (Ti_3Al and TiAl) were also deposited in the close region of the substrate material and a harder coating layer was formed in the middle zone as 670HV. Ti-rich intermetallic hardness value was also determined as high as in our study similarly as 700 HV done by Zhang et al. [15].

3.3 Oxidation Behavior of Aluminized Samples

Although Ti-6Al-4V alloy has good strength and low density it is a candidate material for aerospace industry. However, these superior properties decrease when it is used at high usage temperatures above 300–400 °C [2]. According to a study done by Cimenoglu et al. [16], oxidation at 600 °C for Ti6Al4V alloy resulted in the formation of outer TiO_2 layer.

XRD analysis results of uncoated Ti6Al4V sample at 800 °C can be seen in Fig. 6. For testing the oxidation resistance at higher temperatures, the uncoated Ti-6Al-4V alloy and 700 °C for 4 and 6 h aluminum deposited samples were subjected to oxidation tests in an open atmosphere furnace at 800 °C and at a heating rate of 10 °C/min for 4, 20 and 40 h

Table 2 Parabolic oxide growth rate constants of low temperature aluminized samples

Samples	k_p ($\times 10^{-10}$) ($mg^2 \cdot cm^{-4} \cdot h^{-1}$)
Bare-Ti64	12.23
4 h-Aluminised Ti64	0.216
6 h-Aluminised Ti64	0.154

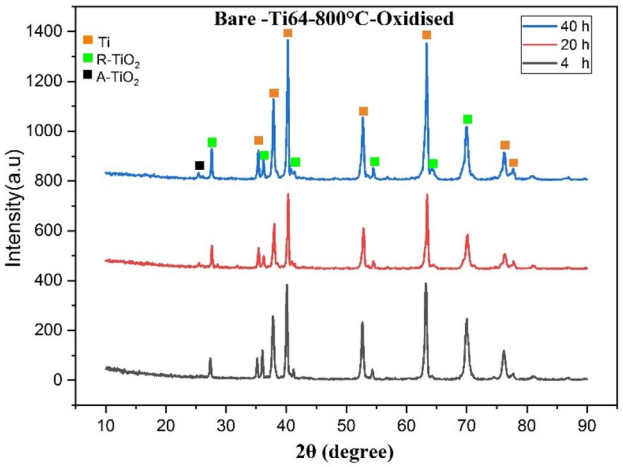

Fig. 6 XRD Analyses of uncoated Ti6Al4V sample oxidised at 800 °C

was subjected to oxidation tests. The weight change method per unit area was used to calculate the oxidation resistance of the samples subjected to oxidation tests. With the formula given in Eq. (1), the oxidation parabolic rate constant (k_p) values of all samples subjected to the oxidation test have been determined [17].

$$(\Delta m/A)^2 = k_p \cdot t \quad (1)$$

Here; Δm is the weight difference, A is the surface area of the sample, and t is the oxidation time. As it seen from Table 2, the highest k_p value was obtained for uncoated Ti64 sample as the lowest parabolic oxidation growth was seen for 6 h coated Ti64 sample. The obtained kp values for Ti64, Ti64-700-4 h, Ti64-700-6 h were 12.23×10^{-10}, 0.216×10^{-10}, 0.154×10^{-10} $mg^2 \cdot cm^{-4} \cdot h^{-1}$ respectively. The Ti64-700-6 h aluminised sample was found to have the maximum oxidation resistance. However, there was no significant difference between the Ti64-700-4 h aluminized sample.

When the Ti6Al4V alloy was exposed to oxidation at 800 °C, a rapid linear mass increase was observed for the sample, Fig. 7. This graph is suitable with the research done by Parekh et al. [2]. They studied; uncoated Thermally treated and Plasma treated Ti6Al4V sample's oxidation behaviour at 600 °C and obtained a similar curve.

The oxide formed on the bare sample surface is based on TiO_2 and tends to grow rapidly.

It was also detected with XRD analyses of bare sample in Fig. 6. In the XRD pattern, "A" represents anatase form and "R" represents oxide in rutile form. Titanium aluminide-based intermetallic coating deposited on the surface, on the other hand, did not show a significant weight increase at 800 °C and remained stable. While almost no deterioration was observed in the coating layer, a thin alumina (Al_2O_3) film deposition was seen on the surface. Because of the very high level aluminum content (of about 65 wt.%), $TiAl_3$ and $TiAl_3$-based intermetallics generally form a protective external alümina-Al_2O_3 layer and have the ability to maintain this scale [17]. The intermetallics are not only known with

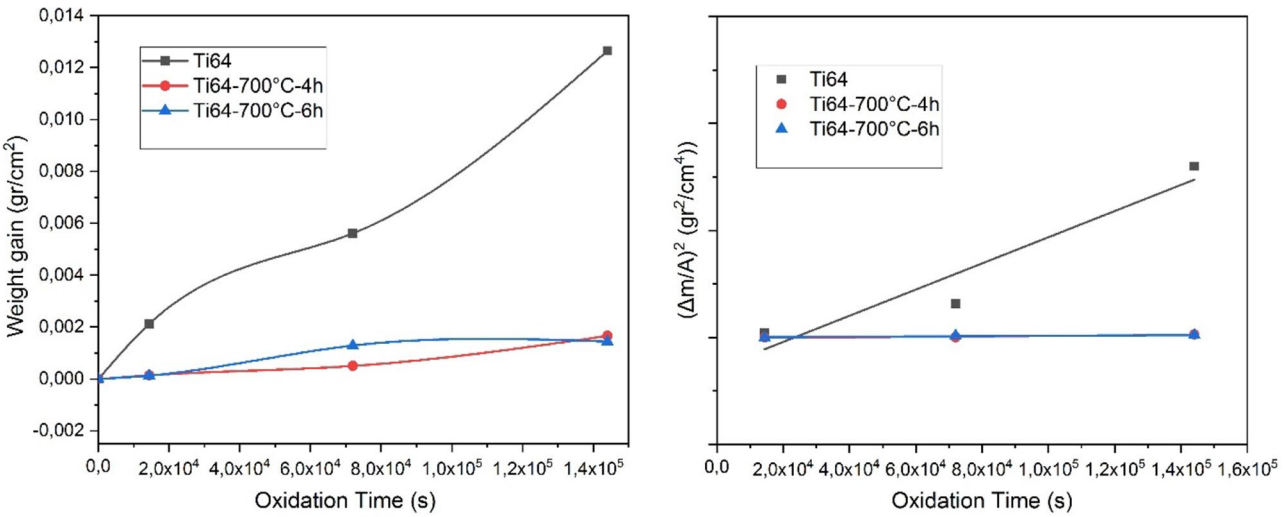

Fig. 7 Oxidation time-dependent (800 °C) **a** weight gain per surface area and **b** rate constant determination graph of oxidized samples

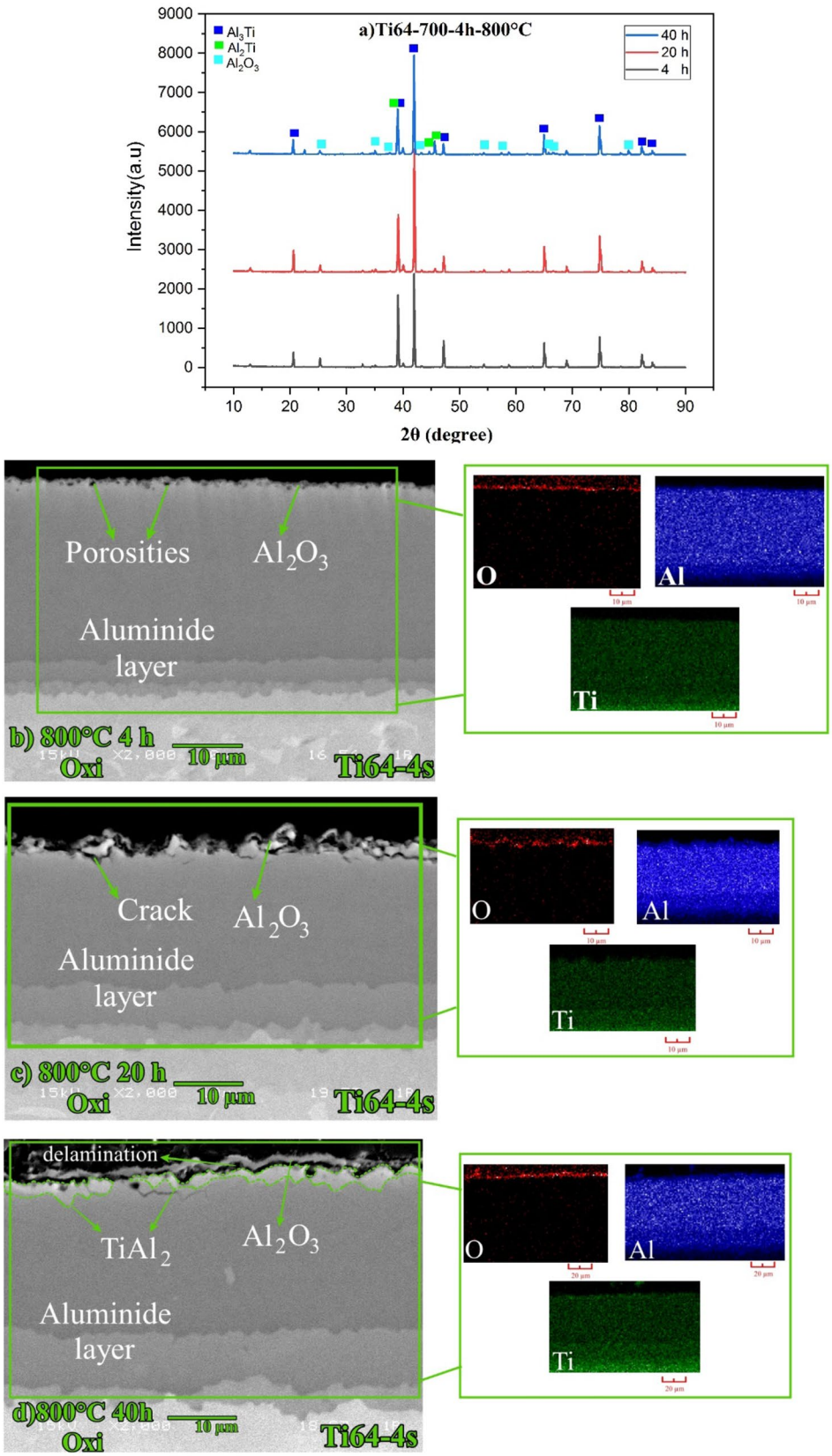

Fig. 8 SEM-MAP Analyses of Ti64-4 h. sample, aluminised at 800 °C

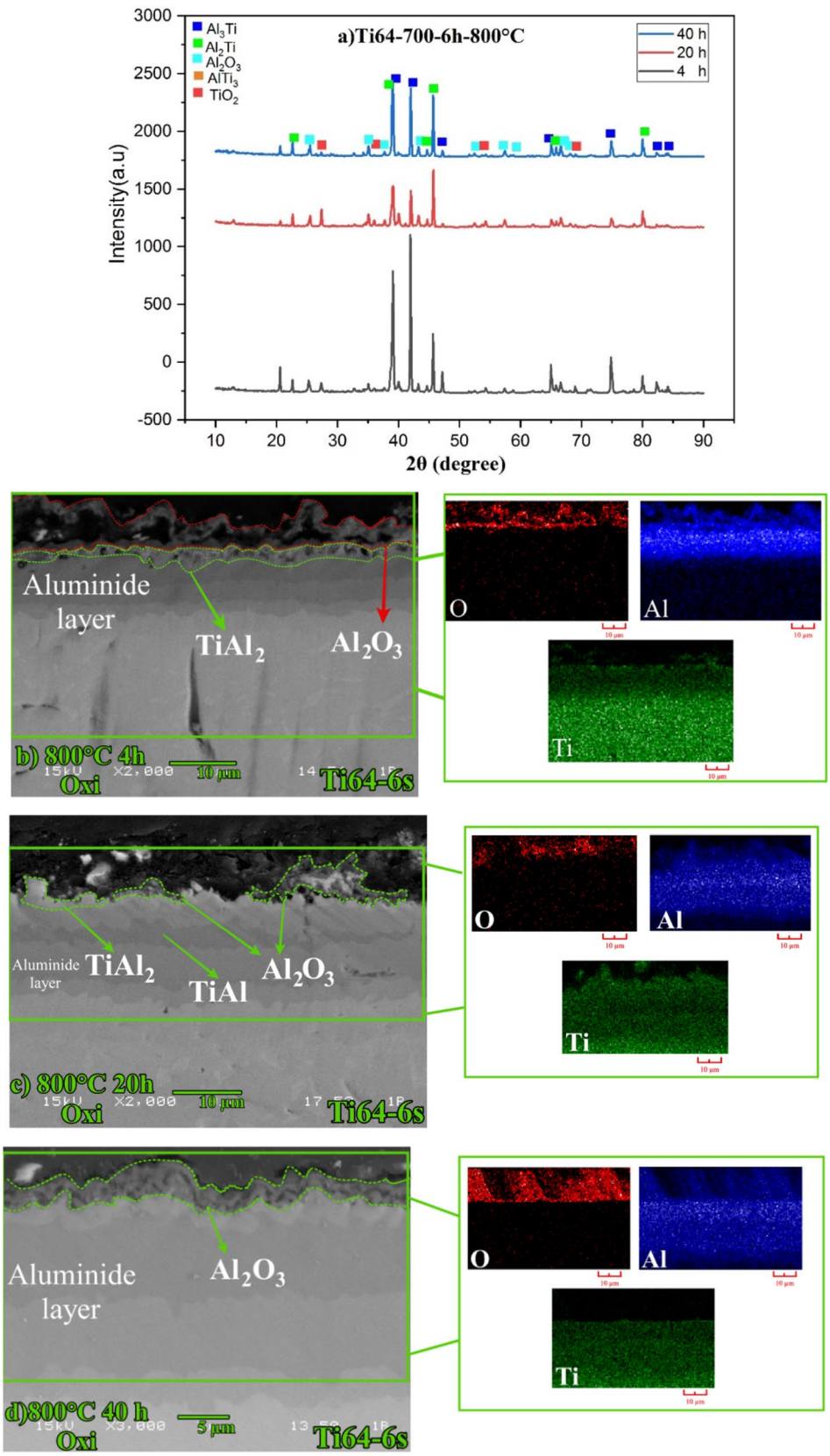

Fig. 9 SEM-MAP Analyses of Ti64-6 h sample, oxidisied at 800 °C

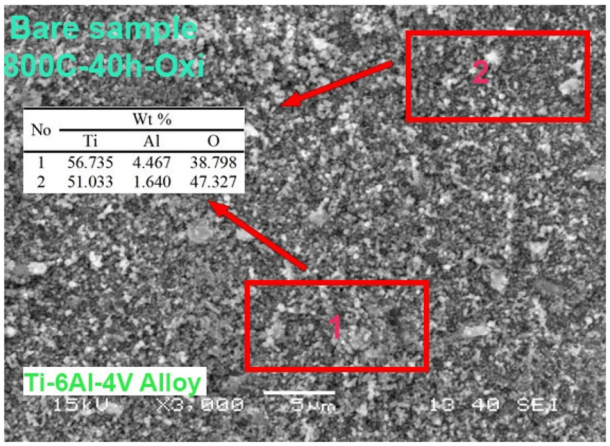

Fig. 10 SEM–EDS Analyses of Bare Ti64-sample surface view of 800 °C-40 h oxidation

its high-temperature resistance properties, but also a good oxidation resistance for the substrate [9, 18]. The increased reactivity of Al during the low-temperature aluminizing process caused inward diffusion of Al and its interaction with Ti, culminating in the creation of $TiAl_3$, which produced the protective aluminized layer. In the initial oxidation process, which started with 4 h at 800 degrees, almost no change was observed on the surface. A slight porous structure started to form on the top surfaces of the intermetallic coating layer. However, at 20 h oxidation, a very thin alumina layer was formed, and at 40 h, aluminum oxidation occurred on the surface, while the aluminum content of the coating decreased and the $TiAl_3$ phase transformed into $TiAl_2$.

Figures 8 and 9 shows XRD and SEM-Mapping analyses results after oxidation test. In Fig. 8, the phases detected on the aluminum-coated sample surface at 700 °C-6 h belonged to the intermetallic phases based on $TiAl_3$ and $TiAl_2$, as well as Al_2O_3. Similarly, when the surface analysis was examined, a thin oxide layer was clearly seen. Depending on the increasing oxidation time, the oxide layer expanded. Looking at Fig. 9, it was determined that the surface of the sample, which was coated with aluminum for 700°-6 h, was rich in Al_2O_3 and the thickness of the oxide layer increased. It is also understood from the weight gain graphs after oxidation that the oxide continued along the surface and provided a protective surface (Fig. 10).

SEM micrographs are given in Fig. 11 after oxidation of Ti64-4 h and Ti64-6 h sample at 800 °C temperature for 4, 20 and 40 h from surface. Outermost surface layer was comprised of Al-rich Ti intermetallic as well as Al_2O_3 after oxidation. When we look at the EDS results increasing with the oxidation time, it could be seen that the oxygen amount on the surface increased. Likewise, according to SEM–EDS images, it could be seen that a stable α-Al_2O_3 layer was formed with the increase of the oxidation time, and plate-like structure was determined on the oxidized sample surfaces. Ti-Al-based intermetallic coatings resulted with a mixture structure of $TiAl_2$ and Al_2O_3 phases up to 40 h oxidation exposure whereas Ti64 bare sample surface consisted of TiO_2 after oxidation at 800 °C. Bare Ti64 alloy surface view after 800 °C-40 h oxidation can be seen in Fig. 10. Surface morphology comprised of totally Ti rich oxide zone.

According to Oxidation kinetics of titanium aluminides [6]; Al_2O_3 and TiO_2 originate at the same time in the initial oxidation state and expand in the same direction. Because the growth activation energy of TiO_2 is substantially lower than that of Al_2O_3, the growth velocity of TiO_2 is much higher than that of Al_2O_3. A titanium oxide layer grows quickly on the surface of the alloys during the ensuing growing process [6].

4 Conclusions

- Pack cementation has been used to deposit aluminide-based intermetallic coatings on Ti6Al4V super alloy at low temperatures. The substrate's microstructure and oxidation characteristics, as well as the generated aluminide layers, have been studied. The following is a brief summary of the study's findings:
- The intermetallic coating formed on the surface via low temperature pack aluminising process at 700 °C 4 and 6 h are essentially three layer structure.
- The hardness values are at about 650 HV and 600 HV for the top coating region of the coating whereas the alloy hardness value is 350HV.
- Oxidation test results show that Ti6Al4V alloy oxidation resistance is highly improved after aluminising process and the surface oxide is aluminium oxide Al_2O_3 contrary to TiO_2 on the bare alloy. The production of alumina as oxide scale during the pack aluminizing process improves the oxidation resistance of Ti6Al4V alloy.

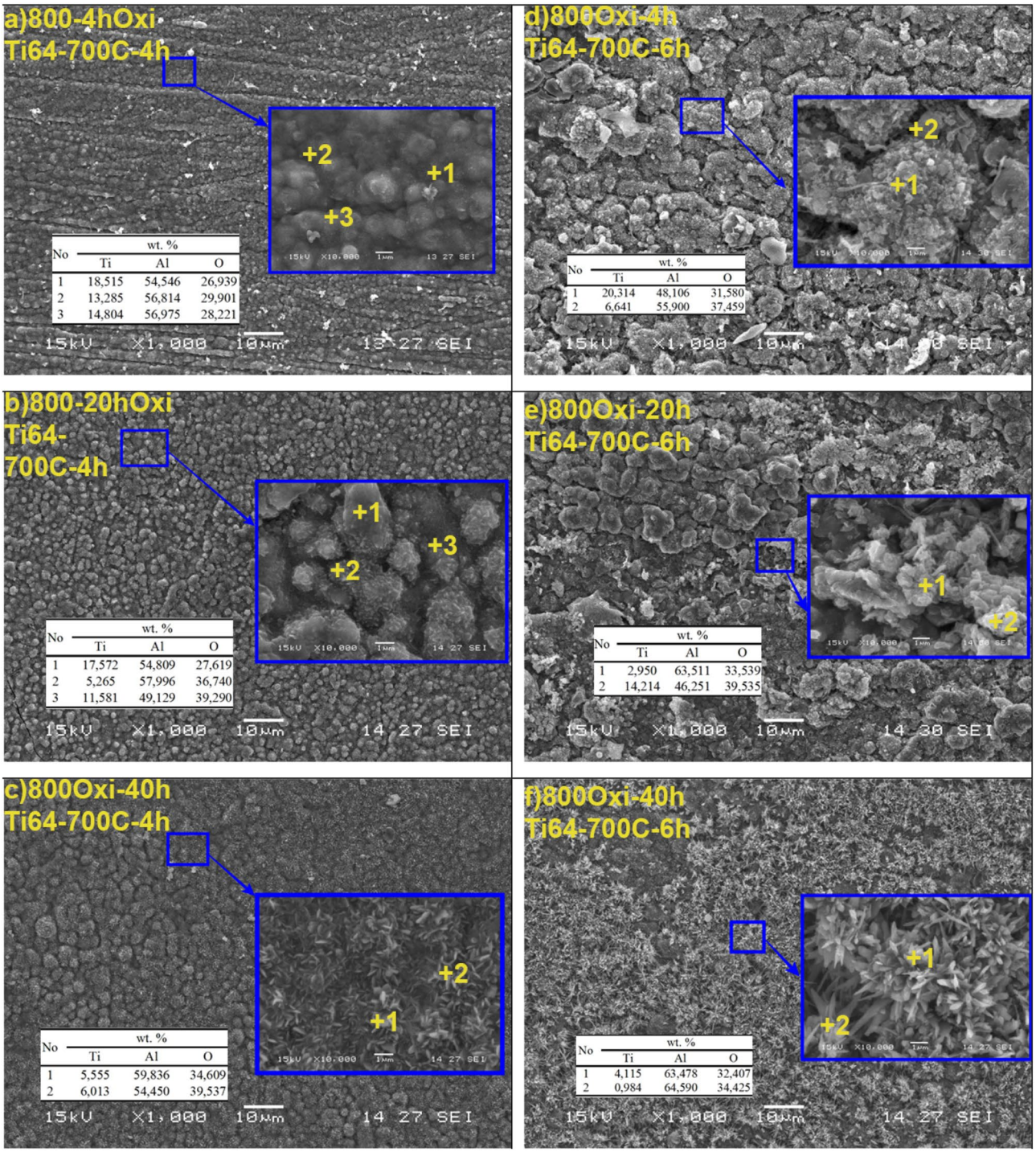

Fig. 11 SEM Analyses of Ti64-700 °C-4 and 6 h samples surface view exposure from 800 °C oxidation

Declarations

Conflict of interest There is no conflict of interest.

References

1. Ayday A, *El-Cezeri J Sci Eng* **7** (2020) 402. https://doi.org/10.31202/ecjse.648678
2. Parekh T, Patel P, Sasmal C S, and Jamnapara N I, *Surf Coat Technol* **394** (2020) 125704. https://doi.org/10.1016/J.SURFCOAT.2020.125704

3. Guleryuz H, and Cimenoglu H, *J Alloys Compd* **472** (2009) 241. https://doi.org/10.1016/j.jallcom.2008.04.024
4. Yang W, Park J, Choi K, Chung C H, Lee J, Zhu J, Zhang F, and Park J S, *Int J Refract Met Hard Mater.* **101** (2021) 105642. https://doi.org/10.1016/j.ijrmhm.2021.105642
5. Chen C, Feng X, and Shen Y, *J Alloys Compd* **813** (2020) 152223. https://doi.org/10.1016/j.jallcom.2019.152223
6. Dai J, Zhu J, Chen C, and Weng F, *J Alloys Compd* **685** (2016) 784. https://doi.org/10.1016/j.jallcom.2016.06.212
7. Döleker K M, Erdogan A, Yener T, Karaoglanlı A C, Uzun O, Gök M S, and Zeytin S, *Surf Coat Technol* **412** (2021) 127069. https://doi.org/10.1016/j.surfcoat.2021.127069
8. Ayday A, Kırsever D, and Demirkıran A Ş, *Trans Indian Inst Met* **75** (2022) 27. https://doi.org/10.1007/s12666-021-02368-6
9. Yener T, *Vacuum* **162** (2019) 114. https://doi.org/10.1016/j.vacuum.2019.01.040
10. Yener T, *Sakarya Univ J Sci* **23** (2019) 817. https://doi.org/10.16984/saufenbilder.495407
11. Celebi Efe G, *Mater Tehnol* **48** (2014) 827.
12. ASM Handbook Corrosion, (1992) Volume 13.
13. Rastkar A R, Parseh P, Darvishnia N, and Hadavi S M M, *Appl Surf Sci* **276** (2013) 112. https://doi.org/10.1016/j.apsusc.2013.03.043
14. Yener T, and Zeytin S, *Mater Tehnol* **48** (2014) 847.
15. Zhang W, Li W, Zhai H, Wu Y, Wang S, Liang G, and Wood R J K, *Surf Coat Technol* **395** (2020) 125944. https://doi.org/10.1016/j.surfcoat.2020.125944
16. Guleryuz H, and Cimenoglu H, *Surf Coat Technol* **192** (2005) 164. https://doi.org/10.1016/j.surfcoat.2004.05.018
17. Okafor I C I, and Reddy R G, *JOM* **51** (1999) 35. https://doi.org/10.1007/s11837-999-0092-9
18. Yener T, Yener S C, and Zeytin S, *Mater Tehnol* **50** (2016) 899. https://doi.org/10.17222/mit.2015.189